View metadata, citation and similar papers at core.ac.uk
brought to you by CORE
provided by Institutional Repository of the Freie Universität Berlin

CdS/Cu(In,Ga)S_2 based solar cells with efficiencies reaching 12.9% prepared by a rapid thermal process

S. Merdes[1*], D. Abou-Ras[1], R. Mainz[1], R. Klenk[1], M. Ch. Lux-Steiner[1], A. Meeder[2], H. W. Schock[1] and J. Klaer[1]
[1]Helmholtz-Zentrum-Berlin für Materialien und Energie, Hahn-Meitner-Platz 1, D14109 Berlin, Germany
[2]Soltecture Solartechnik GmbH, Groß-Berliner Damm 149, D12487 Berlin, Germany

Abstract

In this Letter, we report externally confirmed total area efficiencies exceeding 12.8% for CdS/Cu(In,Ga)S_2 based solar cells. These are the highest reported confirmed efficiencies of CdS/Cu(In,Ga)S_2 based thin film solar cells. The Cu(In,Ga)S_2 absorber was prepared from sputtered metals subsequently sulfurized using rapid thermal processing in sulfur vapor. Basic structural and electrical properties of the devices are presented.

Keywords: Cu(In,Ga)S_2, thin film, solar cell, record efficiency, rapid thermal processing

*Corresponding author.
Email address: saoussen.merdes@helmholtz-berlin.de (S. Merdes)

1. Introduction

In the last decades, investigation of wide gap chalcopyrite materials, in particular $CuInS_2$ (CIS), has grown considerably. The interest in these materials is beyond the laboratory scale. Application and technology scale up have already been introduced by companies such as Soltecture, which established a pilot production of CIS based thin film solar modules in Berlin [1]. According to Shockley and Queisser's calculations, the maximum conversion efficiency that a single junction solar cell can achieve would be from an absorber material with a band gap ranging between 1.2 to 1.4 eV [2]. Therefore, CIS is expected to lead theoretically to higher solar cell efficiencies, compared with what has been achieved experimentally so far, if we consider its band-gap energy of 1.5 eV which is close to optimum. However, CdS/$CuInS_2$ based solar cells still suffer from a low open-circuit voltage. Incorporation of gallium has led to a significant improvement in device performance. A CdS/Cu(In,Ga)S_2 based solar cell with an efficiency of 11.2% was reported by Watanabe and Matsui [3], and Jahagirdar et al. [4] achieved a confirmed efficiency of 12% by optimizing the thickness of the i-ZnO layer in a Cu(In,Ga)S_2 based device where the absorber was prepared by the sulfurization of metallic precursors in H_2S. Recently, our group reported a Cu(In,Ga)S_2 solar cell showing an efficiency of 12.6% together with an open-circuit voltage of 879 mV confirmed by NREL [5]. Based on previous investigations [5-8], we have further modified the baseline process for the growth of Cu(In,Ga)S_2 (CIGS) absorbers. In the present Letter, we report CIGS based solar cells with record efficiencies exceeding12.8% certified by the Fraunhofer Institute (ISE) and achieved after that modification.

2. Absorber growth and device fabrication

An In/(Cu,Ga) precursor layer stack was deposited by DC magnetron sputtering on Mo-coated float glass substrates. In/(Cu,Ga) refers to a layer of In followed by a layer sputtered from a (Cu,Ga) alloy target. The layer stack was characterized by an integral [Ga]/([In]+[Ga])

ratio of 0.26 and a [Cu]/([In]+[Ga]) ratio of 1.50. Further details about precursor preparation are described elsewhere [8, 9]. The sputtered layers were heated together with elemental sulfur, which was provided as granules, in a quartz enclosure by radiation from halogen lamps. Precursors were preannealed in the chamber. Then, the sulfurisation was carried out at nominal temperatures of about 560 ºC for 3 min. An additional high temperature phase, a few seconds at 630 °C, was introduced here with the aim of promoting the interdiffusion of the In-rich and Ga-rich ternary phases [9]. This interdiffusion (which is mandatory for good device performance) was previously achieved by higher dwell temperatures, but those were problematic with regard to glass softening, molybdenum layer stress and homogeneity over larger areas [5, 7, 8]. Cu_xS forms on CIGS during sulfurization and is removed by KCN etching. After the absorber growth and the etching, the solar cells were completed by depositing the CdS buffer layer and a transparent ZnO/ZnO:Al window layer. Finally, Ni-Al grids were evaporated. The solar cells received a MgF_2 anti-reflection coating.

3. Device characterization

In Fig. 1 the current-voltage $I(V)$ characteristics of a champion CIGS based solar cell, prepared as described above, are presented. The measurement was performed at the Fraunhofer ISE calibration laboratory. For an area of 0.54 cm^2, a confirmed efficiency (η) of (12.8±0.4)% was achieved. The solar cell shows an open-circuit voltage (V_{oc}) of (814±4) mV, a short-circuit current density (J_{sc}) of (22.7±0.6) mA/cm^2 and a fill factor (FF) of (69.0±0.7)%. Compared to our previously confirmed efficiency of 12.6% [5], this sample shows an improved photocurrent collection and consequently a higher J_{sc}. The dark $I(V)$ characteristics were fitted using the single diode model. A diode ideality factor A of 1.9, a saturation current density J_o of about 4 x 10^{-7} mA/cm^2, a series resistance R_s of 0.8 Ω $cm^2$and a shunt resistance R_{sh} of 1.2 kΩ cm^2 were extracted.

Temperature dependent current-voltage measurements $I(V,T)$ were carried out between 150 and 320 K to investigate recombination mechanisms in the device. The dark and light temperature dependencies of the ideality factor are shown in Fig. 2 (a). Under illumination, the ideality factor A is below 2 and is temperature independent, which indicates a thermally activated recombination mechanism. However, in the dark, the diode ideality factor is temperature dependent which is typical for a tunneling dominated recombination process. An open circuit voltage of 1.3 V at 0 K is extrapolated from the plot of the open circuit voltage as function of temperature [10] shown in Fig. 2 (b). Recombination in the bulk should result in a V_{oc} (0 K) ≈ 1.53 V corresponding to the band gap of the absorber. Interface recombination gives however a V_{oc} (0 K) = E_b/q [11] where E_b is the effective recombination barrier height and q the elementary charge. For our cell, V_{oc} (0 K) ≈ 1.30 V which is smaller than the band gap energy indicating therefore that the device is limited by interface recombination, as previously found in our CIGS based solar cells [12, 13].

The elemental distributions in and the microstructure of CIGS were investigated. Fig. 3 (a) and (b) show the scanning electron microscopy (SEM) image and electron backscatter diffraction (EBSD) pattern quality map, respectively, whereas Fig. 4 (a) shows energy dispersive X-ray (EDX) elemental distribution maps all acquired at the identical position of the new record efficiency solar cell. The SEM cross-section image shows a very rough absorber surface with depressions reaching 700 nm. Large voids close to the back-contact, which have been found previously in our CIGS samples [7] are also visible. They are probably caused by outdiffusion of material to the surface during the growth of the chalcopyrite. The EBSD map shows clearly a dual microstructure of the CIGS absorber with two distinct layers composed of several grains with different orientations visible from the corresponding EBSD orientation distribution map, not shown here. The grain sizes are significantly smaller in the bottom layer and vary between 0.5 and 1 μm whereas they reach 2 μm in the upper layer. In

Fig. 4 (a) the EDX elemental distribution maps were acquired using an acceleration voltage of 7 kV. The signals of the Si-K, Mo-L, Ga-L, In-L, Cd-L and Zn-L lines are given superposing a SEM image. The layered structure of the CIGS absorber is apparent, where the Ga-rich phase remains at the back of the CIGS layer while the In-rich one is located close to the CdS/ZnO layers [14]. However, here interdiffusion has clearly taken place between $CuGaS_2$ (CGS) and CIS as evidenced by the colored patterns. The layered structure results from the growth kinetics of CIGS (prepared by a sequential process) where CIS and CIG are formed separately at slightly different points in time [5, 6, 9]. CIGS forms only later in the process by the interdiffusion of CIS and CGS [9].

In Fig. 4 (b), the EDX elemental distribution profiles extracted from the maps in Fig. 4 (a) are plotted against the CIGS layer depth. We focus here on the Cu, In, Ga and S distributions. The position of the Mo and CdS buffer layer are indicated in the figure. Note that since the S related signals include the signature of the CdS buffer layer, it extends 50 nm beyond the absorber thickness. The gallium concentration is highest close to the back contact and decreases gradually towards the surface. However, gallium is still detected unambiguously in the CIGS adjacent to the CdS layer. Taking into account a signal broadening of about 300 nm due to the electron excitation at 7 keV, the width of the interdiffusion zone between the In-rich phase and the Ga-rich phase is estimated to be 1 μm. A gallium content of about 3-4 at.% is detected in the part of the absorber adjacent to the CdS layer. This supports the assumption of increase in band-gap energy at the top of the absorber compared with that of pure CIS. In Fig. 5, the gallium distribution profile of the 12.8% efficient solar cell is plotted together with that of our previous best solar cell [5] with an efficiency of 12.6%, an open circuit voltage of 879 mV, a short circuit current of 20.4 mA/cm^2 and a fill factor of 70%. One can see clearly that the two cells show a different gallium distribution profile through the absorber thickness. Both absorbers show a double graded like Ga/(Ga+In) ratio profile with a Ga/(Ga+In) ratio of 0.06 and 0.30 at the surface for the 12.8% and 12.6% efficient cell respectively.

In Fig. 6 (a) are plotted the external quantum efficiencies (EQE) of the 12.6% and 12.8% efficient cells in addition to the quantum efficiency of a reference solar cell with an efficiency of 7.8%, an open circuit voltage of 657 mV, a short circuit current of 20.2 mA/cm^2 and a fill factor of 59%. The reference solar cell absorber was prepared using the experimental conditions described in this work however the additional high temperature step was omitted for comparison. One can see clearly that the reference solar cell has a much lower quantum efficiency not exceeding 80% compared to the champion cells. A shift is also observed in the blue region of the spectrum for the reference sample. This shift is, however, merely due to using the conventional undoped ZnO (i-ZnO) in the window layer instead of Zn(Mg, O) as in the champion cells. The band-gap of the absorber in the reference cell was estimated from the first derivation of the EQE as function of photon energy and was found to be 1.50 eV. This points to a layered structure of the absorber, with $CuInS_2$ at the top and $CuGaS_2$ at the bottom, and proves the efficiency of the additional heating step, that was introduced to the process described in this work, in promoting the interdiffusion between the Ga-rich and In-rich ternary phases. The 12.8% efficient solar cell shows a better current collection between 500 and 800 nm compared to the 12.6% efficient solar cell. It also shows that the 12.8% efficient solar cell has a steeper absorption edge indicating a better current collection in the red region side. This suggests that the two absorbers have a different Ga distribution through the thickness as shown by the EDX elemental distribution profiles in Fig. 5 . In Fig 6 (b) are plotted the resulting simulated external quantum efficiencies of the 12.8% and 12.6% efficient solar cells using the program SCAPS [15]. The typical parameters for CIGS based solar cells were kept constant except the gallium grading within the absorbers which was varied according to the depth profiles shown in Fig. 5. The vacuum level was kept constant and the valence band edge of the absorbers was graded below band-gap energies of

1.75 eV in both solar cells. The simulated solar cell characteristics are gathered in table1. The solar cell with the absorber prepared using the old process gives a much larger open circuit voltage of 1081 mV and a lower short circuit current compared with those of the sample prepared using the modified process which is consistent with the larger amount of gallium at the absorber surface as measured by EDX. The back grading seems however insufficient to result in a higher current collection. While it is difficult to carry out a full statistical analysis for a laboratory scale process, where the number of cells is limited and where the parameters are changed frequently, the characteristics of our best externally certified solar cells prepared using the old and modified process are gathered in table 1. One can see that the samples prepared using the old process show a higher open circuit voltage reaching 882 mV whereas the ones prepared using the modified process show either a better current collection or a better fill factor as demonstrated by the simulations. Note that an efficiency of 12.9% was achieved 17 months after the 12.8% efficiency obtained using the modified process. These two solar cells which are characterized by a rather good current collection or fill factor support the hypothesis that an optimum gallium distribution profile is mandatory for high efficiencies.

Recently, low band-gap $Cu(In,Ga)Se_2$ based solar cells have achieved an efficiency of 20.3% [16]. The question what limits the efficiency of the sulfide based cells compared to the selenide ones is a very pressing issue and an unambiguous theory would greatly enhance our understanding of chalcopyrite-based cells. The different Cu-stoichiometry and the etching treatment are one significant difference between the sulfide and the selenide cells and may well be one reason for the different dominant recombination mechanism [12, 17]. On the other hand, it is well known that the very high efficiency of selenide cells can be maintained only up to a certain band gap of the absorber. If, after the recent improvements of the sulfide cells, we now compare them to selenide cells with the same wide band gap there is no longer a significant difference in performance [18]. This suggests that the absorber band-gap has a stronger influence on the performance than the Cu stoichiometry and the etching.

4. Summary

We presented CIGS based solar cells with efficiencies reaching 12.9% prepared using a modified baseline process. These are the higher externally confirmed efficiencies for sulphide based solar cells. These devices show a different gallium distribution profile compared with the old process that results in a higher current collection or fill factor.

Acknowledgments

The authors would like to thank B. Bunn, C. Kelch and M. Kirsch for the preparation of the solar cells and J. Schniebs for the deposition of the anti-reflection layer. M. Burgelman is gratefully acknowledged for providing the simulation program SCAPS and the BMU for the financial support (0327589A and 0327589B.

References

[1] Neisser A, Meeder A, Zetzsche F, Rühle U, von Klopmann C, Stroh R, Meyer N. Manufacturing of large-area $CuInS_2$ solar modules- From pilot to mass production: Proceedings of the 24th European Photovoltaic Solar Energy Conference, Hamburg 2009; 2460-2464

[2] Shockley W, Queisser H J. Detailed balance limit of efficiency of p-n junction solar cells. J. Appl. Phys. 1961; **32**: 510-519.

[3] Watanabe T, Matsui M. Improved efficiency of $CuInS_2$-based solar celles without potassium cyanide process. Jpn. J. Appl. Phys. 1999; **38**: L 1379-L 1381

[4] Jahagirdar A H, Kadam A A, Dhere N G. Role of i-ZnO in optimizing open circuit voltage of $CIGS_2$ and CIGS thin film solar cells: Proceedings of the 4th World Conference on Photovoltaic Energy Conversion, Waikoloa 2006; 557-559
[5] Merdes S, Mainz R, Klaer J, Meeder A, Rodriguez-Alvarez H, Schock H W, Lux-Steiner M Ch, Klenk R. 12.6% efficient CdS/Cu(In,Ga)S_2 based solar cell with an open circuit voltage of 879 mV prepared by a rapid thermal process. Sol. Energy Mater. Sol. Cells 2011; **95**: 864-869
[6] Mainz R, Klenk R, Lux-Steiner M Ch. Sulphurisation of gallium-containing thin-film precursors analysed in-situ. Thin Solid Films 2007; **515**: 5934-5937
[7] Merdes S, Kaigawa R, Klaer J, Klenk R, Mainz R, Meeder A, Papathanasiou N, Abou-Ras D, Schmidt S. Increased open circuit voltage in Cu(In,Ga)S_2 based solar cells prepared by rapid thermal processing of metal precursors: Proceedings of the 23rd European Photovoltaic Solar Energy Conference, Valencia 2008; 2588-2591
[8] Mainz R, Klaer J, Klenk R, Papathanasiou N. Solar cells based on Cu(In,Ga)S_2 prepared by a two-step process. Proceedings of the 22nd European Photovoltaic Solar Energy Conference, Milan 2007; 2429-2433
[9] Merdes S, Mainz R, Rodriguez-Alvarez H, Klaer J, Klenk R, Meeder A, Schock H W, Lux-Steiner M Ch. Influence of precursor stacking on the absorber growth in Cu(In,Ga)S_2 based solar cells prepared by a rapid thermal process. Thin Solid Films 2011; **519**: 7189-7192
[10] Nadenau V, Rau U, Jasenek A, Schock H W. Electronic properties of $CuGaSe_2$-based heterojunction solar cells. Part I. Transport analysis. J. Appl. Phys. 2000; **87**: 584-593
[11] Klenk R. Characterization and modelling of chalcopyrite solar cells. Thin Solid Films 2001; **387**: 135-140
[12] Merdes S, Sáez-Araoz R, Ennaoui E, Klaer J, Lux-Steiner M Ch, Klenk R. Recombination mechanisms in highly efficient thin film Zn(S,O)/Cu(In,Ga)S_2 based solar cells. Appl. Phys. Lett. 2009; **95**: 213502
[13] Riedel I, Riediger J, Ohland J, Keller J, Knipper M, Parisi J, Mainz R, Merdes S. Photoelectric characterization of Cu(In,Ga)S_2 solar cells obtained from rapid thermal processing at different temperatures., Sol. Energy Mater. Sol. Cells 2011; **95**:270-273
[14] Mainz R, Streicher F, Abou-Ras D, Sadewasser S, Klenk R, Lux-Steiner M Ch. Combined analysis of spatially resolved electronic structure and composition on a cross-section of a thin film Cu($In_{1-x}Ga_x$)S_2 solar cell. Phys. Status Solidi A 2009; **206**: 1017-1020
[15] Burgelman M, Verschraegen J, Degrave S, Nollet P. Modeling thin-film PV devices. Prog. Photovolt: Res. Appl. 2004; **12**: 143-153
[16] Jackson P, Hariskos D, Lotter E, Paetel S, Wuerz R, Menner R, Wischmann W, Powalla M. New world record efficiency for Cu(In,Ga)Se_2 thin-film solar cells beyond 20%. Prog. Photovolt: Res. Appl. 2011; **19**: 894-897
[17] Rau U. Tunneling-enhanced recombination in Cu(In,Ga)Se_2 heterojunction solar cells. Appl. Phys. Lett. 1999; **74**: 111-113
[18] Klenk R, Klaer J, Köble Ch, Lux-Steiner M. Ch, Mainz R, Merdes S, Rodriguez Alvarez H, Scheer R, Schock H W. Development of $CuInS_2$-based solar cells and modules. Sol. Energy Mater. Sol. Cells 2011; **95**: 1441-1445

Figure captions

Fig. 1. $I(V)$-characteristics of a CIGS based solar cell prepared by a sequential process as described in the text. The measurement was performed at the Fraunhofer ISE calibration lab. The data are: η = 12.8%, V_{oc} = 814 mV, J_{sc} = 22.7 mA/cm^2, FF = 69%, area = 0.54 cm^2.

Fig. 2. (a). Temperature dependence of the diode ideality factor. (b). Temperature dependence of the open-circuit voltage.

Fig. 3. (a). SEM image acquired on a cross-section of the solar cell. (b). EBSD pattern quality map taken from the same area.

Fig. 4. (a). EDX elemental distribution maps acquired on the cross-section of the sample. (b). Elemental distribution profiles of Cu, In, Ga and S extracted from the elemental distribution maps in (a) and plotted against the absorber layer depth, measured at the same area.

Fig. 5. Depth profiles of the 12.8 % and 12.6% efficient solar cells showing the relative Ga content along the absorber thickness.

Fig. 6. (a) Comparison of the experimental external quantum efficiency of the 12.8% and the 12.6% efficient best solar cells. (b) Simulated external quantum efficiencies of the 12.8% and 12.6% efficient solar cells.

Table 1: The resulting simulated solar cell characteristics calculated for the 12.8% and 12.6% efficient solar cells using the gallium distribution profiles represented in Fig.5. O: refers to the old baseline process described in [5]. M: refers to the modified baseline process described in this work.

Sample	**Process**	**Voc (mV)**	**Jsc (mA/cm^2)**	**FF (%)**	**η (%)**
1717-68-5	O	1081	19.1	58	12.0
1689-38-5	M	897	23.7	73	15.4

Table 2: Summary of the best externally certified solar cells. O: refers to the old baseline process described in [5]. M: refers to the modified baseline process described in this work.

Sample	**Certification date**	**Process**	**Voc (mV)**	**Jsc (mA/cm^2)**	**FF (%)**	**η (%)**
1717-68-5	29.06.2010/ NREL	O	879	20.4	71	12.6
1717-68-4	29.06.2010/ NREL	O	882	21.1	70	12.5
1689-38-5	16.04.2010/ ISE	M	814	22.7	69	12.8
2727-12-7	22.09.2011/ ISE	M	835	21.2	73	12.9

Fig. 1

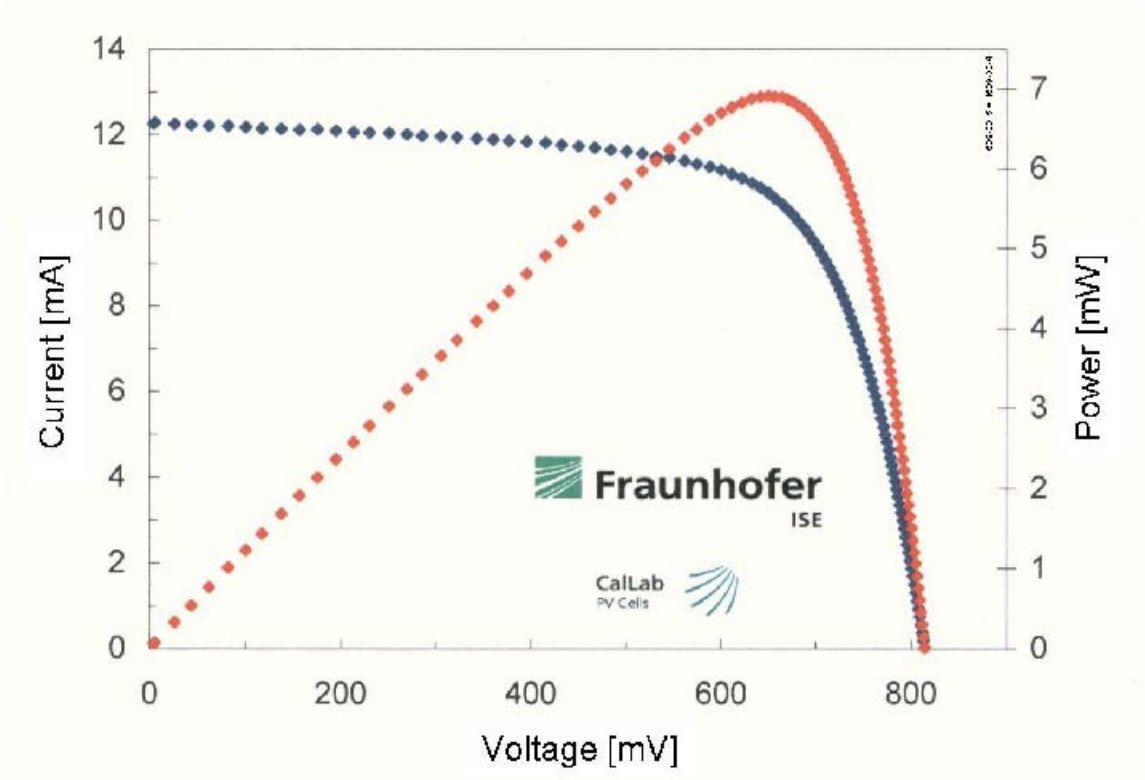
Current [mA]
Power [mW]
Voltage [mV]
0
2
4
6
8
10
12
14
0
1
2
3
4
5
6
7
0
200
400
600
800
Fraunhofer
ISE
CalLab
PV Cells

Fig. 2

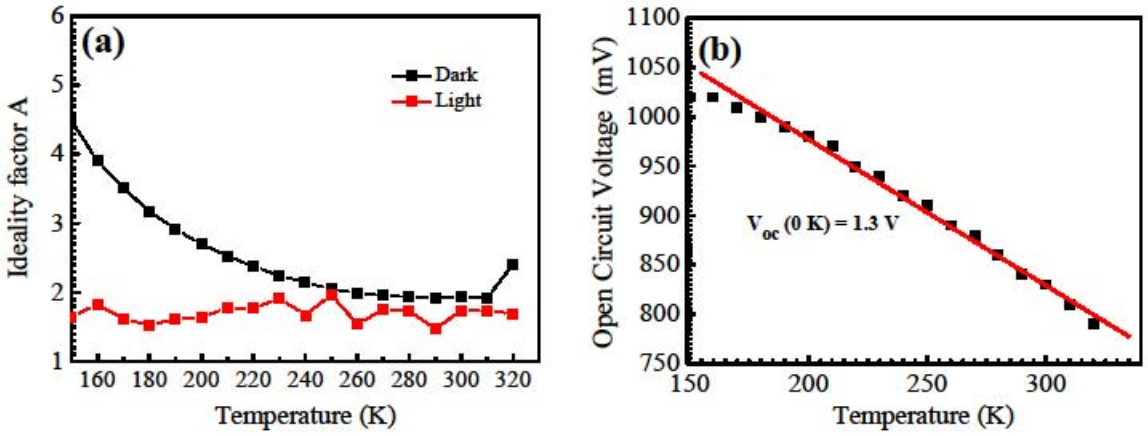
(a)
Dark
Light
Ideality factor A
Temperature (K)
(b)
Open Circuit Voltage (mV)
V_{oc} (0 K) = 1.3 V
Temperature (K)

Fig. 3

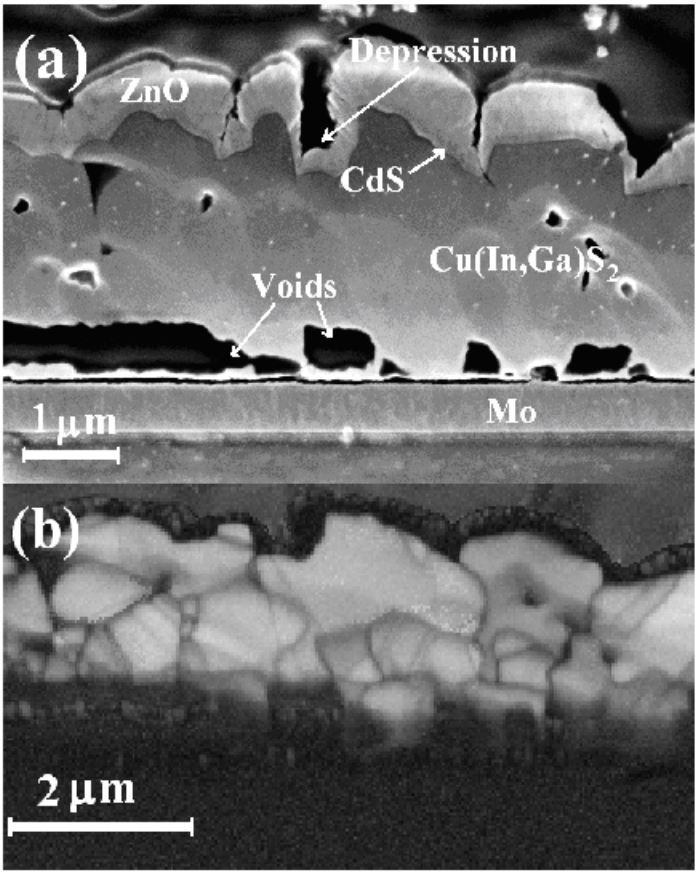

Fig. 4

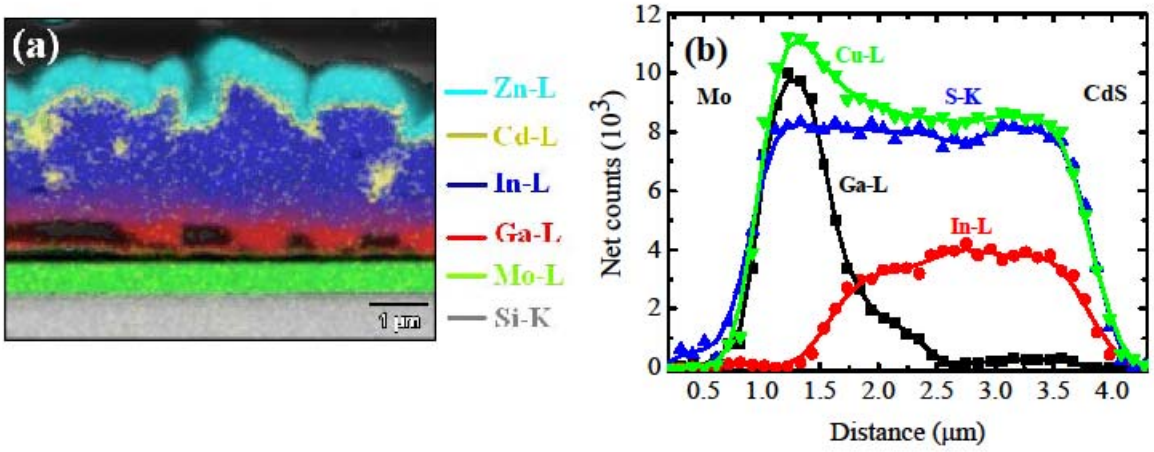
(a)
Zn-L
Cd-L
In-L
Ga-L
Mo-L
Si-K
1 μm
(b)
Mo
Cu-L
S-K
CdS
Ga-L
In-L
Net counts (10^3)
Distance (μm)
0
2
4
6
8
10
12
0.5
1.0
1.5
2.0
2.5
3.0
3.5
4.0

Fig. 5

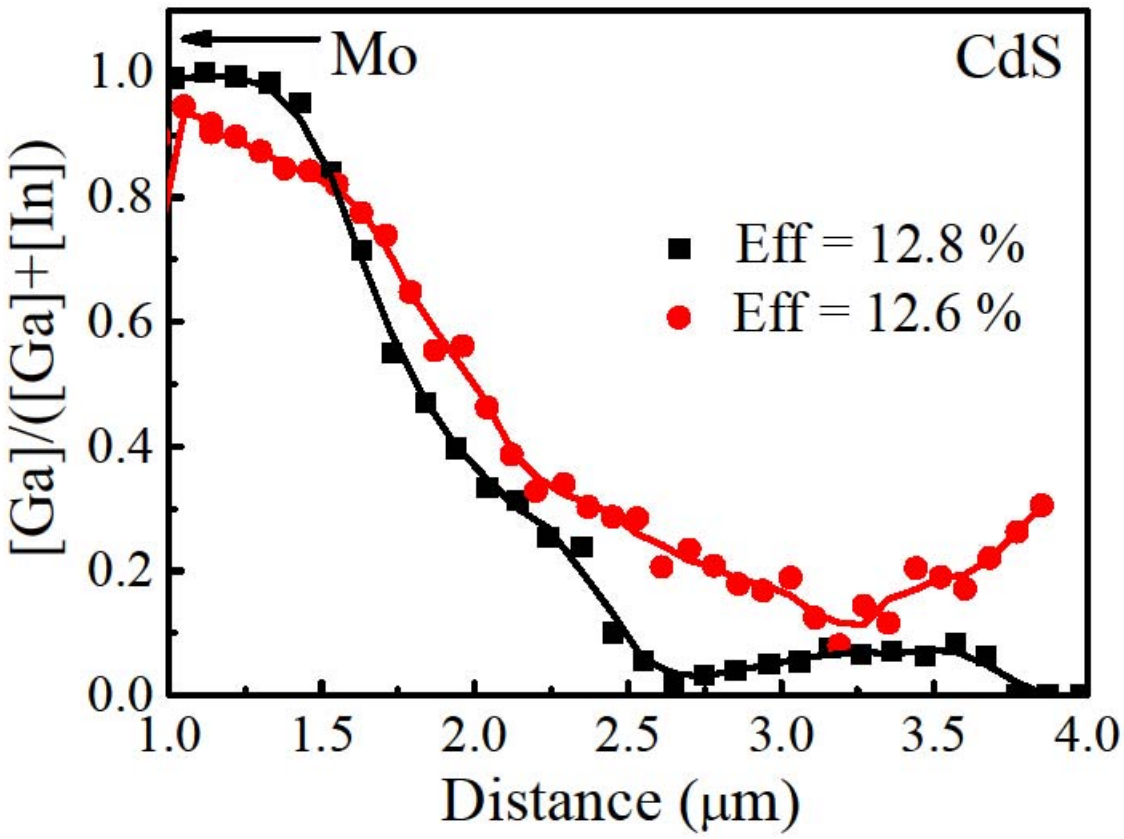
Mo
CdS
Eff = 12.8 %
Eff = 12.6 %
[Ga]/([Ga]+[In])
Distance (μm)
0.0
0.2
0.4
0.6
0.8
1.0
1.0
1.5
2.0
2.5
3.0
3.5
4.0

Fig. 6

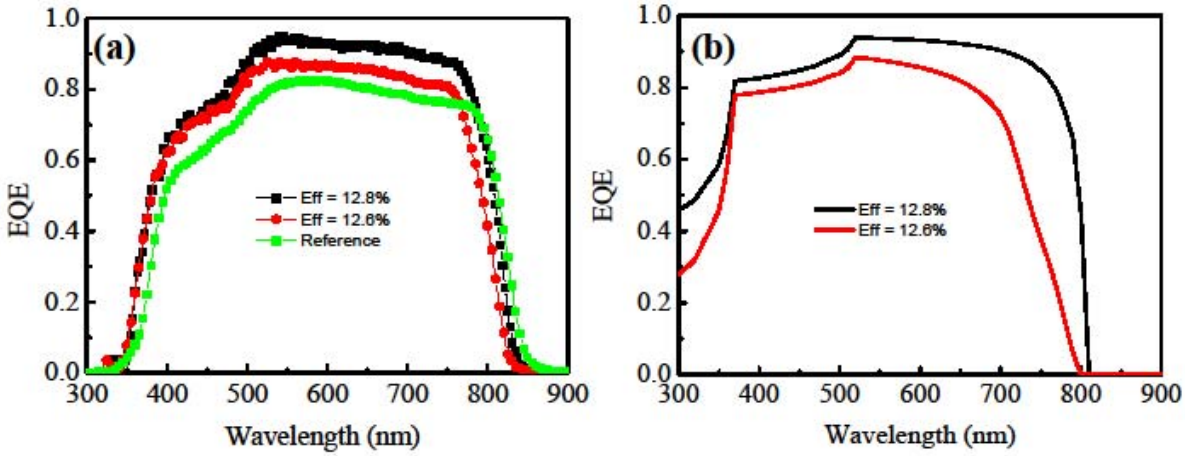
(a)
EQE
Wavelength (nm)
Eff = 12.8%
Eff = 12.6%
Reference
(b)
EQE
Wavelength (nm)
Eff = 12.8%
Eff = 12.6%